BEAM DYNAMICS STUDIES OF THE 8 GeV LINAC AT FNAL*

P.N. Ostroumov†, B. Mustapha, ANL, Argonne, IL 60439 USA

J.-P. Carneiro‡, FNAL, Batavia, IL 60510, U.S.A.

Abstract

The proposed 8-GeV proton driver (PD) linac at FNAL includes a front end up to ~420 MeV operating at 325 MHz and a high energy section at 1300 MHz. A normal conducting RFQ and short CH type resonators are being developed for the initial acceleration of the H-minus or proton beam up to 10 MeV. From 10 MeV to ~420 MeV, the voltage gain is provided by superconducting (SC) spoke-loaded cavities. In the high-energy section, the acceleration will be provided by the International Linear Collider (ILC)-style SC elliptical cell cavities. To employ existing, readily available klystrons, an RF power fan out from high-power klystrons to multiple cavities is being developed. The beam dynamics simulation code TRACK, available in both serial and parallel versions, has been updated to include all known H-minus stripping mechanisms to predict the exact location of beam losses. An iterative simulation procedure is being developed to interact with a transient beam loading model taking into account RF feedback and feedforward systems.

INTRODUCTION

Fermilab is developing the design for a high intensity proton driver 8 GeV superconducting (SC) H⁻ linac. The principal mission of this proton driver (PD) linac is to increase the intensity of the Fermilab Main Injector for the production of neutrino superbeams. There are many other possible applications such as fixed target programs or acceleration of other species (e-, p, μ, etc…) as discussed in ref. [1] and [2].

To make the overall project cost-effective, the general approach was to adopt designs from existing accelerator or proposals. In particular we propose [3]:

- To directly apply the International Linear Collider (ILC) RF system (cavities, cryomodules and klystrons) operating at 1.3 GHz to accelerate the beam from 1.2 GeV to 8 GeV.
- To use Squeezed ILC (S-ILC) cavities operating at 1.3 GHz and designed for β_G=0.81 to accelerate the beam from ~420 MeV to 1.2 GeV.
- To operate the whole linac with only 2 frequencies in order to simplify the RF system. The front-end of the linac provides acceleration up to ~420 MeV operating at 325 MHz, the 4th sub-harmonic of the ILC frequency.

The front-end of this linac, up to 60 MeV, is currently being built by the High Intensity Neutrino Source (HINS)

R&D Program to demonstrate some of the novel design concepts [4]. In the paper we discuss the beam dynamics design of the PD linac.

LAYOUT OF THE FNAL PD LINAC

Based on the design published in 2006 [3], the proposed linac has the characteristics listed in Table 1. A schematic layout of the accelerator is shown in Fig. 1 together with the transport line to the Main Injector.

Table 1: Basic Parameters of the Linac

Parameters	Value
Particle type (baseline mission)	H⁻
Beam kinetic energy	8 GeV
Beam current avg. over the pulse	25 mA
Beam current upstream of the chopper	43 mA
Pulse repetition rate	10 Hz
Pulse length	1 msec
Number of protons per pulse	$1.56 \cdot 10^{14}$
Beam pulsed power	200 MW
Beam average power	2 MW
Wall power (estimate)	12.5 MW
Total length	~678 m

Choice of Accelerating Structure

As depicted in Fig. 1, the H⁻ beam from the Ion Source is bunched and accelerated to 2.5 MeV by a Radio-Frequency Quadrupole (RFQ, [5]) operating at 325 MHz. At that energy, a Medium Energy Beam Transport (MEBT) provides the space for a fast beam chopper (<2 ns) that eliminates unwanted bunches and forms an optimal beam time structure for injection into the Main Injector. This chopping decreases the beam average current over the 1 msec pulse from ~45 mA to ~25 mA. Acceleration to ~100 MeV could be provided by Room temperature DTL cavities; however, a different approach was selected. Taking advantage of the development and excellent performance of SC Spoke cavities [6], it was decided to accelerate the beam from ~10 MeV to ~420 MeV using SC Single and Triple Spoke resonators (SSR and TSR). The Spoke resonators not only present the advantages of higher accelerating gradients and cost-effective operation but also allow one single klystron to power several cavities with the use of high-power ferrite vector modulators [7]. With this outstanding feature of the FNAL PD, only five J-PARC type 2.5 MW klystrons
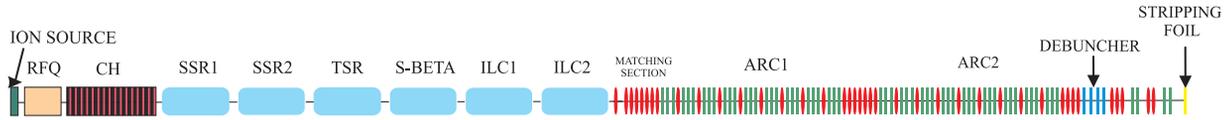
Figure 1: Schematic layout of the FNAL PD linac and High Energy Beam Transport to the Main Injector

Table 2: Main Parameters for each Section of the FNAL PD Linac with Focusing Type (S: Solenoid, R: Resonator, nR: n Resonators, F: Focusing quad. and D: Defocusing quad)

Section No.	Section Name	Wout (MeV)	Cavities No.	Focusing Type	Period No.	Lf (m)	z (m)
1	CH	10	16	S1R	16	0.49- 0.75	17
2	SSR1	32	18	S1R	18	0.75	31.4
3	SSR2	124	33	S2R	18	1.6	61.0
4	TSR	421	42	FRDR	21	3.8	142.2
5	S-ILC	1223	56	F2RD2R	14	6.1	226.7
6	ILC1	2445	63	F4RD3R	9	12.2	336.5
7	ILC2	8000	224	F8RD8R	14	24.2	678.1
Total		8000	452		110		~678

are necessary to power the entire 420-MeV front-end of the linac. To boost the beam from 2.5 MeV to 10 MeV it was decided to use room-temperature cross-bar H-type (CH) cavities which have a higher shunt impedance (90 MOhm/m to 60 MOhm/m) than DTLs. Cavities of this type have been developed by Frankfurt University [8] as an accelerating structure for the future GSI proton synchrotron. For this energy range SC cavities are not an option as time-consuming and expensive development of several types would be required. Furthermore, the number of lattice transitions in the linac directly corresponds to the number of cavity types and must be minimized. As previously mentioned final acceleration to 8 GeV is provided by S-ILC and ILC type 1.3 GHz cavities. The frequency transition occurs at high energy (~420 MeV) which is favorable to the longitudinal beam dynamics.

Choice of Focusing Structure

In the front-end, between the RFQ and TSR sections, SC solenoid magnets were selected as focusing elements for the following reasons:

- Axially-symmetric beam is less sensitive to space charge effects and helps mitigate the formation of halo (especially in the MEBT where long drifts are necessary to accommodate the chopper).
- Solenoids provide shorter length of the focusing period relative to quadrupole FODO which facilitates the use of the higher gradient offered by SC cavities.
- Solenoids can be made with bucking coils and do not require any additional shielding in the vicinity of the SC resonators. This results in a compact lattice which is very important in the low energy section.

Above ~100 MeV, focusing is provided with FODO quadrupole focusing. At these energies, the beam is less sensitive to spaces between the linac components and, moreover, focusing with ~6 T solenoids can result in stripping of the H^- beam in the fringe fields.

The different sections of the linac with corresponding main parameters are presented in Table 2. The linac is made of 110 focusing periods with lengths varying from 49 cm to 24.2 m. As depicted in Fig. 1, the beam is transferred from the linac to the Main Injector by a High Energy Beam Transport (HEBT), a regular FODO lattice (60° phase advance per cell) made of two opposite sign arcs. A matching section with 6 transverse collimators is located upstream of the first arc and 4 debuncher cavities (necessary to reduce the momentum spread) downstream of the second arc. Downstream of the debuncher, the beam enters a matching section to get the desired beta function at the stripping foil. The total length of the linac and the transport line is ~1.7 km.

LATTICE DESIGN

The design of the PD linac lattice has been performed following general design requirements for a high-intensity proton linac necessary to avoid RMS emittance growth [3]:

- The zero current phase advance of transverse and longitudinal oscillations should be kept below 90° per focusing period to avoid parametrically-excited instabilities at high current.
- The transverse and longitudinal wavenumbers k_{x0}, k_{y0}, k_{z0} must change adiabatically along the linac. This feature minimizes the potential for mismatches and

helps assure a current independent lattice. The wavenumbers of particle oscillations are expressed as

$$k_{T0} = \frac{\sigma_{T0}}{L_f}, \quad k_{L0} = \frac{\sigma_{L0}}{L_f}, \quad \text{where} \quad \sigma_{T0}, \quad \sigma_{L0} \text{ are}$$

the zero current transverse and longitudinal phase advances per focusing period of length L_f.

- Avoid the $n=1$ parametric resonance between the transverse and longitudinal motion. The condition for occurrence of an n-th order transverse motion parametric resonance is $\sigma_{T0} = \frac{n}{2}\sigma_{L0}$. The strongest resonance is for n=1 and can occur particularly in SC linacs due to the availability of high accelerating gradients and relatively long focusing periods. It can be avoided by proper choice of operational tunes in the Kapchinskiy stability diagram.
- Avoid strong space charge resonances by selecting stable areas in the Hofmann's stability chart [9].
- Provide beam equipartitioning to avoid energy exchange between the transverse and longitudinal planes that can occur via space-charge forces.
- Provide proper matching in the lattice transitions to avoid appreciable halo formation.

In NC linacs these requirements can be fulfilled for peak currents up to ~150 mA [10]. Cost-effective SC linac solutions are more challenging. For example, cavities and focusing elements in SC linacs are combined into relatively long cryostats with an ineluctable drift space between them. Also there is a sharp change in the period length at transitions between the linac sections of different cavity types.

BEAM DYNAMICS SIMULATIONS

The main tool used for the design of the PD linac is the code TRACK [11]. For benchmarking purposes the simulations have also been performed with the DESY code ASTRA [12]. Simulations presented in this paper start at the RFQ exit.

Figure 2 shows TRACK and ASTRA simulations of the PD linac at zero current. The transverse and longitudinal phase advances depicted in Fig. 2(a) present some strong but innocuous jumps due to changing length of the focusing periods at transitions between different types of cavities. Aside from few periods, the transverse and longitudinal phase advances are kept below 90°. The smooth evolution of the transverse and longitudinal wavenumbers shown in Fig. 2(b) is achieved by properly selecting the length of the focusing periods (as shown in Table 2) and adequately adjusting the synchronous phase φ_s of each cavity. Figure 3 shows the voltage gain per cavity. The Kapchinskiy stability diagram (Fig. 2(c)) presents the evolution of $cos(\sigma_T)$ as a function of the defocusing factor γ_s for each one of the 110 periods. The gray area shows the boundary for the $n=1$ parametric resonance to occur. The dashed line corresponds to the stability required for the particles near the separatrix boundary at a phase angle of $-2|\varphi_s|$. The majority of the
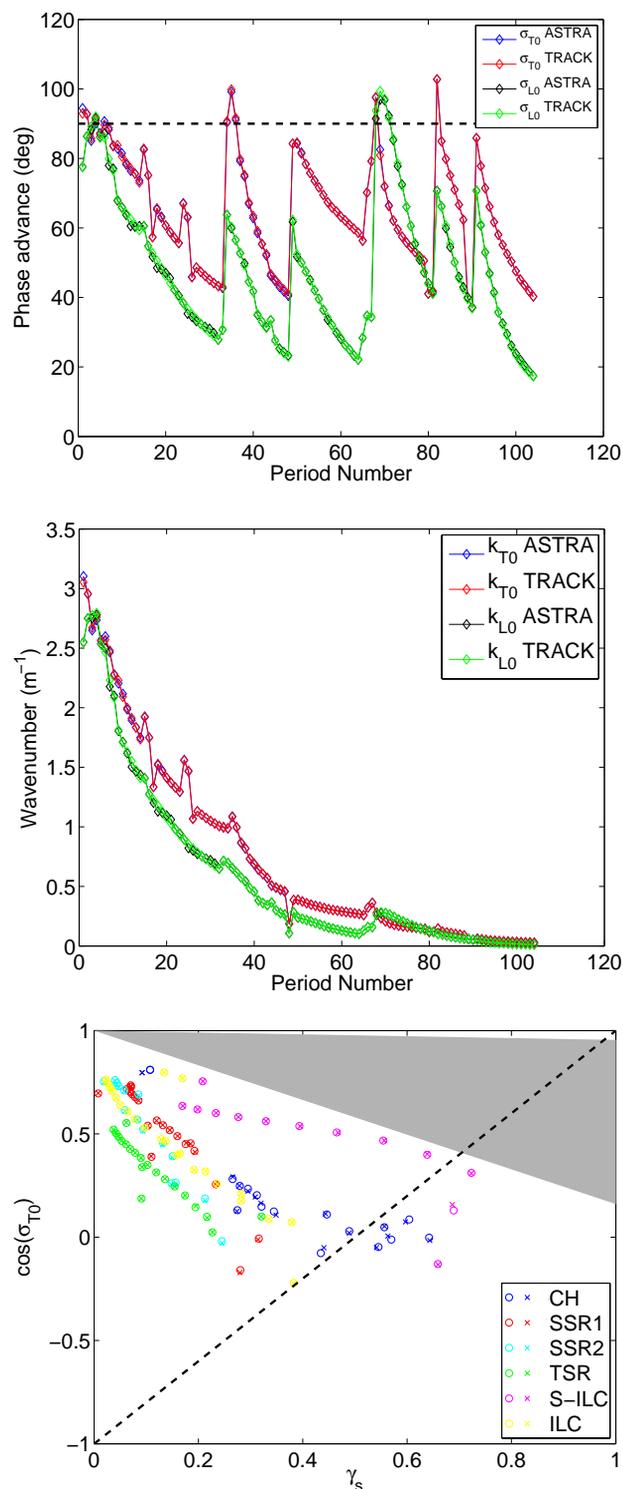

Figure 2: TRACK and ASTRA simulations of the FNAL PD linac at zero current: (a) trans. and long. phase advances, (b) trans. and long. wavenumbers and (c) Kapchinskiy stability diagram. The gray area in (c) shows the boundary of the $n=1$ parametric resonance and the dashed line corresponds to the stability of particles located near the separatrix. In (c) the circles crosses represent TRACK and ASTRA, respectively.
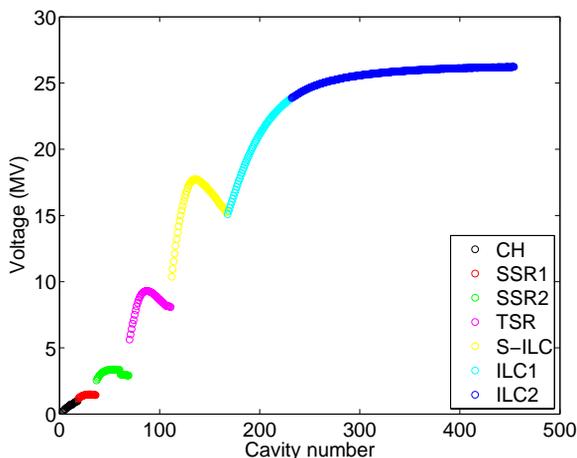
Figure 3: Voltage gain per cavity.

operating tunes are located in stable regions with few points lying on unstable ones. These tune points correspond to matching sections and are not expected to affect the beam since the susceptibility to instability exists for only a short distance compared to the betatron oscillation wavelength. Figure 4 presents Hofmann's stability chart (for details on the chart see for instance [13]) for the PD linac at the design current of 43 mA with a longitudinal to transverse emittance ratio of $\varepsilon_L/\varepsilon_T=2$.
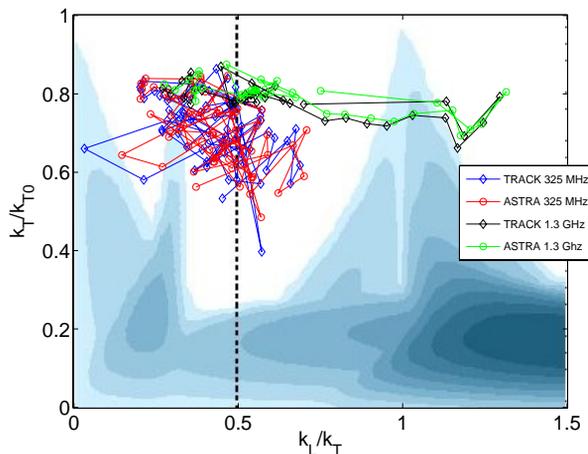

Figure 4: Hofmann's chart for a long. to trans. emittance ratio of 2. Courtesy of I. Hofmann.

As depicted on Fig. 4, both TRACK and ASTRA predict a moderate tune depression (0.5-0.8) along the linac with most of the operating tunes laying on stable (white) areas or fast-crossing the resonances. Therefore, space charge driven resonances are not a concern for this linac design.

Emittance Growth and Beam Losses

Figure 5 shows TRACK and ASTRA simulations of the RMS transverse and longitudinal emittance growth factor along the PD linac at 43 mA. These are acceptable levels and are mainly attributed to imperfect matching between the different lattice transitions. Detailed beam loss studies along the PD linac have been performed with TRACK using 10^8 macro-particles. Results are reported in Ref.

[14]. These studies concluded that for typical values of misalignments and RF errors ($\pm1°$ and $\pm1\%$ RMS) the PD linac produces very limited total and peak power losses, respectively at 1×10^{-4} and ~0.04 W/m for the linac operating at ~25 mA ($1.56\cdot10^{14}$ ppp) and 10 Hz.
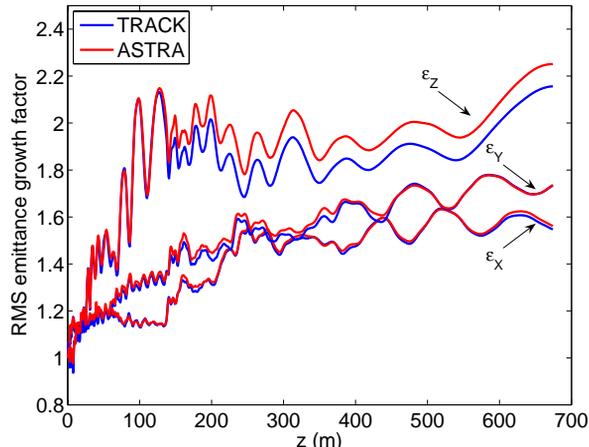

Figure 5: RMS trans. and long. emittance growth factor along the FNAL PD linac at 43 mA.

Large Scale Computing with PTRACK

A parallel version of TRACK, PTRACK is being implemented on the BG/P supercomputer at ANL. With a 3D domain decomposition parallel Poisson solver, PTRACK can run on BG/P using more than 10^4 processors. A novel advantage of this large scale computing is the possibility to perform simulations with a number of particles that equals the population of the bunch. A detailed description of PTRACK is presented in ref. [15]. Figure 6 shows a PTRACK simulation of the PD linac and HEBT with 10^8 macro-particles on 4k processors and a total time of ~6.5 hours. PTRACK has successfully simulated 865 M (real bunch population for the current design of 43 mA) on the FNAL RFQ using 32k processors for a total time of ~6 hours. Start-to-end simulations with 865 M macro-particles are in progress and represent an ideal tool for studies of beam losses or halo formation.
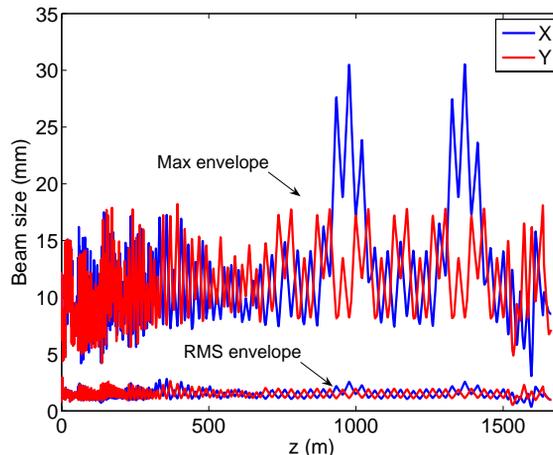

Figure 6: PTRACK simulation of beam envelope along the FNAL PD linac and HEBT at 43 mA with 10^8 p.

H⁻ Stripping Simulations

A potential source of uncontrolled losses in H⁻ linacs is the stripping of the H⁻ ion. H⁻ ions have two electrons, one tightly bound at 13.6 eV binding energy and one loosely bound at 0.75 eV. During acceleration and transport, the ions suffer from blackbody radiation, electromagnetic fields, and residual gas any of which can strip the loosely bound electron. To quantify stripping losses, all three of these mechanisms have been recently implemented in the code PTRACK. A compilation of the H⁻ stripping equations as implemented in the code is presented in ref. [16]. The code allows the user to set the temperature, pressure, and composition of the residual gas for any desired section of the linac. Concerning the residual gas, TRACK now supports stripping from H_2, O_2, Xe, Ar, He, Ne. CO_2, CO, H_2O will be implemented soon in the code.

Figure 7 presents PTRACK simulation of the stripping losses along the PD linac using 10^8 macro-particles. For these simulations, typical temperature and pressure along the linac were setup in the code: SC linac (from SSR to ILC) at 4 K, 1×10^{-10} T and the transport line at 150 K, 5×10^{-9} T. Only H_2 has been considered as the residual gas for these simulations. Losses were computed for an average beam current of ~25 mA and 10 Hz. Figure 7 reports that for these conditions, the stripping losses along the linac remain below 0.1 W/m. Combined with the typical RF and misalignment errors previously mentioned, the peak power losses along the PD linac and HEBT remain below 0.1 W/m. This represents a safe margin from the 1W/m loss criterion widely adopted by the accelerator community.

LLRF Transient Analysis

A new analytical approach is being developed to simulate LLRF system and determine optimized set point for the cavity operation in an RF unit where each cavity operates at a specific synchronous phase, accelerating field and under heavy beam loading. This method is
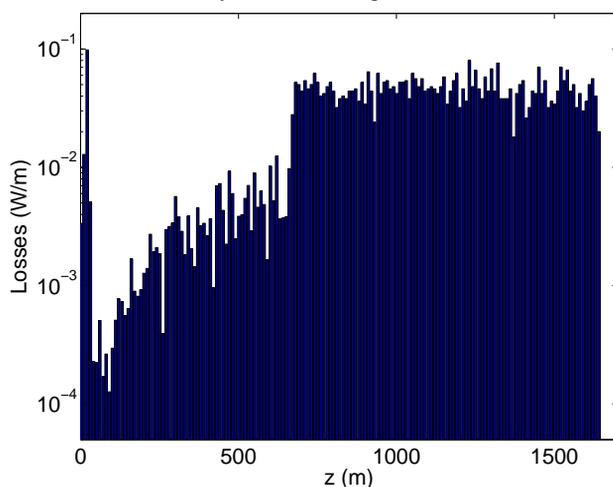

Figure 7: PTRACK simulation of the stripping losses along the FNAL PD linac and HEBT for typical operation.

described in ref. [17] and based on the cavity transient response in the presence of various imperfections, feedforward and feedback systems. It is our goal to implement the residual errors of the accelerating field parameters along the beam pulse into the TRACK code.

CONCLUSION

The simulated beam dynamics of the ~1.7 km FNAL 8 GeV PD SC linac and transport line show an excellent behavior of the current design in terms of emittance growth and beam losses. High-statistics simulations, with typical machine errors and H⁻ stripping, show very low beam losses (<0.1W/m) along the linac and HEBT. Work is in progress to optimize the high energy section of the linac. Further development of PTRACK will include a realistic LLRF model and will enable even more precise beam dynamics simulations using the real bunch population.

REFERENCES

[1] G.W. Foster and J.A. MacLachlan, "A multi-mission 8 GeV injector linac as a Fermilab booster replacement'', LINAC02.

[2] G.W. Foster (ed.), available at: http://protondriver.fnal.gov/#Technical_Design_Link

[3] P.N. Ostroumov, New J. of Physics, 8, 281, 2006.

[4] R.C. Webber et al. "Overview of the High Intensity Neutrino Source Linac R&D Program at Fermilab'', LINAC08.

[5] P.N. Ostroumov et al., J. of Inst., P04002, 2006.

[6] K. W. Shepard, P. N. Ostroumov, and J. R. Delayen, Phys. Rev. ST – AB 6, 080101, 2003.

[7] R.L. Madrak et al., "A Fast Chopper for the Fermilab High Intensity Neutrino Source (HINS)'', LINAC08.

[8] Z. Li, "Design of the RT CH-Cavity and Perspectives for a new GSI Proton Linac'', LINAC04.

[9] I. Hofmann, Phys. Rev. E 57, 4713, 1998.

[10] G.P. Lawrence and T.P. Wangler, "Integrated Normal-Conducting/Superconducting High Power Proton Linac for APT Project'', PAC97.

[11] V.N. Aseev et al. "TRACK : The new beam dynamics code'', PAC05.

[12] K. Floettmann, ASTRA user manual available at : http://www.desy.de/~mpyflo/Astra_dokumentation/

[13] F. Gerigk, "Space charge and beam halos in Proton Linacs'', US-CERN-JAPAN-RUSSIA Accelerator School, November 2002.

[14] P.N. Ostroumov et al., "Beam dynamics studies of the 8-GeV superconducting H– linac'', LINAC06.

[15] J. Xu et al. "Simulations of high-intensity beams using BG/P supercomputer at ANL'', HB2008.

[16] J.-P. Carneiro, FNAL Beams-doc 2741, April 2007.

[17] G. Cancelo and A. Vignoni, "Optimizing cavity gradients in pulses linacs using the cavity transient response'', LINAC08.